Article

Asymmetric Aza-Henry Reaction Under Phase Transfer Catalysis: An Experimental and Theoretical Study

Enrique Gomez-Bengoa, Anthony Linden, Rosa Lo#pez, Idoia Mu#gica-Mendiola, Mikel Oiarbide, and Claudio Palomo

J. Am. Chem. Soc., **2008**, 130 (25), 7955-7966 • DOI: 10.1021/ja800253z • Publication Date (Web): 30 May 2008

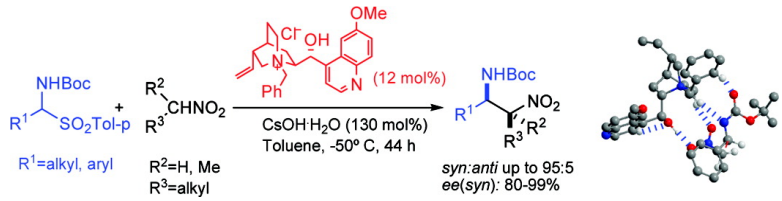

More About This Article

Additional resources and features associated with this article are available within the HTML version:

- Supporting Information
- Links to the 3 articles that cite this article, as of the time of this article download
- Access to high resolution figures
- Links to articles and content related to this article
- Copyright permission to reproduce figures and/or text from this article

View the Full Text HTML

J|A|C|S
ARTICLES

Published on Web 05/30/2008

Asymmetric Aza-Henry Reaction Under Phase Transfer Catalysis: An Experimental and Theoretical Study

Enrique Gomez-Bengoa, Anthony Linden,† Rosa López, Idoia Múgica-Mendiola, Mikel Oiarbide, and Claudio Palomo*

Departamento de Química Orgánica I, Facultad de Química, Universidad del País Vasco, Apdo. 1072, San Sebastián, 20080, Spain

Received January 15, 2008; E-mail: claudio.palomo@ehu.es

Abstract: An efficient catalytic asymmetric aza-Henry reaction under phase transfer conditions is presented. The method is based on the reaction of the respective nitroalkane with α-amido sulfones effected by $CsOH \cdot H_2O$ base in toluene as solvent and in the presence of cinchone-derived ammonium catalysts. This direct aza-Henry reaction presents as interesting features its validity for both nonenolizable and enolizable aldehyde-derived azomethines and the tolerance of nitroalkanes, other than nitromethane, for the production of β-nitroamines. The synthetic value of the methodology described is demonstrated by providing (a) a direct route for the asymmetric synthesis of differently substituted 1,2-diamines and (b) a new asymmetric synthesis of γ-amino α,β-unsaturated esters through a catalytic, highly enantioselective formal addition of functionalized alkenyl groups to azomethines. Finally, a preferred TS that nicely fits the observed enantioselectivity has been identified. Most remarkable, an unusual hydrogen bond pattern for the catalyst-nitrocompound-imine complex is predicted, where the catalyst OH group interacts with the NO_2 group of the nitrocompound.

Introduction

Among the existing methods for the synthesis of nitrogen-containing molecules, the aza-Henry (or nitro-Mannich) reaction is of prime importance.[1] The resulting β-nitroamines can be either oxidized, producing α-amino carbonyl compounds,[2] or reduced, affording 1,2-diamines.[3] Most significant, by this reaction, both nitrogen functionalities, the amino and the nitro groups, are arranged with simultaneous formation of the new C−C bond while the relative and absolute configurations are all fixed in a single synthetic operation. To date, however, the full implementation of this strategy, with high degrees of stereocontrol and substrate tolerance, is far from being satisfactorily solved. Important progress has been made in the catalytic enantioselective aza-Henry reaction of aromatic azomethines based on chiral Lewis acid catalysts of ytterbium,[4] aluminum,[5] copper,[6] zinc[7] metals, and also organocatalysts.[8] Regarding substrate variation in the methods described in literature, some general restrictions remain. Nitroalkane partner is most often restricted to nitromethane or nitroethane, both relatively cheap and volatile, which allows their use in large excess or even as (co)solvent. Longer chain and functionalized nitroalkanes have been scarcely explored.[9] In addition, although the reactions involving nitromethane do not display *syn/anti* isomerism, all other nitroalkanes can produce both diastereomers, an issue poorly solved in the general context of the aza-Henry and the related Henry reaction.[10] On the other hand, the vast majority of the known methods deal with azomethine components derived from nonenolizable aldehydes,[11] typically aromatic *N*-acyl and *N*-phosphinoyl imines or iminoesters. The

† X-ray crystal structure analysis. Organich-chemisches Institut der Universität Zürich, Winthertherstrasse 190, CH-8057 Zürich, Switzerland.

(1) For recent racemic versions, see: (a) Bernardi, L.; Bonini, B. F.; Capitò, E.; Dessole, G.; Comes-Francini, M.; Fochi, M.; Ricci, A. *J. Org. Chem.* **2004**, *69*, 8168–8171. (b) Anderson, J. C.; Blake, A. J.; Howell, G. P.; Wilson, C. *J. Org. Chem.* **2005**, *70*, 549–555. For a highlight disclosing recent catalytic asymmetric approaches, see: (c) Westermann, B *Angew. Chem., Int. Ed.* **2003**, *42*, 151–153.

(2) Reviews on the Nef reaction: (a) Pinnick, H. W. *Org. Reac.* **1990**, *38*, 655–792. (b) Ballini, R.; Petrini, M. *Tetrahedron* **2004**, *60*, 1017–1047. For the synthesis of fine chemicals from nitroalkanes, see: (c) Ballini, R.; Palmieri, A.; Righi, P. *Tetrahedron* **2007**, *63*, 12099–12121.

(3) Lucet, D.; Le Gall, T.; Mioskowski, C. *Angew. Chem., Int. Ed.* **1998**, *37*, 2580–2627.

(4) Yamada, K.; Harwood, S. J.; Gröger, H.; Shibasaki, M. *Angew. Chem., Int. Ed.* **1999**, *38*, 3504–3506.

(5) Yamada, K.; Moll, G.; Shibasaki, M. *Synlett* **2001**, 980–982.

(6) (a) Knudsen, K. R.; Risgaard, T.; Nishiwaki, N.; Gothelf, K. V.; Jørgensen, K. A. *J. Am. Chem. Soc.* **2001**, *123*, 5843–5844. (b) Nishiwaki, N.; Knudsen, K. R.; Gothelf, K. V.; Jørgensen, K. A. *Angew. Chem., Int. Ed.* **2001**, *40*, 2992–2995. (c) Knudsen, K. R.; Jørgensen, K. A. *Org. Biomol. Chem.* **2005**, *3*, 1362–1364. (d) Handa, S; Gnanadesikan, V.; Matsunaga, S.; Shibasaki, M *J. Am. Chem. Soc.* **2007**, *129*, 4900–40091. (e) Zhou, H.; Peng, D.; Qin, B.; Hou, Z.; Liu, X.; Feng, X. *J. Org. Chem.* **2007**, *72*, 10302–10304.

(7) (a) Palomo, C.; Oiarbide, M.; Halder, R.; Laso, A.; López, R. *Angew. Chem., Int. Ed.* **2006**, *45*, 117–120. (b) Trost, B. M.; Lupton, D. W *Org. Lett.* **2007**, *9*, 2023–2026.

(8) (a) Nugent, B. M.; Poder, R. A.; Johnston, J. N *J. Am. Chem. Soc.* **2004**, *126*, 3418–3419. Bifunctional thioureas: (b) Okino, T.; Nakamura, S.; Furukawa, T.; Takemoto, Y. *Org. Lett.* **2004**, *6*, 625–627. (c) Xu, X.; Furukawa, T.; Okino, T.; Miyabe, H.; Takemoto, Y. *Chem.−Eur. J.* **2006**, *12*, 466–476. (d) Yoon, T. P.; Jacobsen, E. N. *Angew. Chem., Int. Ed.* **2005**, *44*, 466–468. Alkaloids: (e) Bernardi, L.; Fini, F.; Herrera, R. P.; Ricci, A.; Sgarzani, V. *Tetrahedron* **2006**, *62*, 375–380. *N*-Sulfinyl ureas: (f) Robak, M. T.; Trincado, M.; Ellman, J. A. *J. Am. Chem. Soc.* **2007**, *129*, 15110–15111.

(9) For some examples of addition of long chain or functionalized nitroalkanes, see refs 5, 6b, d, 7b, 8c, d, and 8f.

(10) Lecea, B.; Arrieta, A.; Morao, I.; Cossío, F. P. *Chem.−Eur. J.* **1997**, *3*, 20–28.

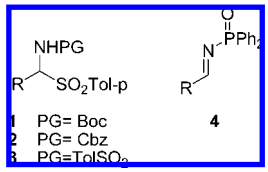

Figure 1. Imine precursors and *N*-phosphinoyl imine employed in this study.

Scheme 1. Aza-Henry Reaction of Nitromethane with Azomethines Generated from α-Amido Sulfones **1** under PTC

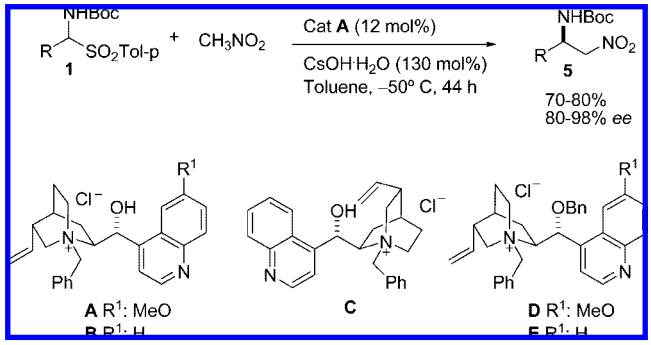

reason is that enolizable aldehyde-derived azomethines tend to suffer α-deprotonation rather than addition. Apart from these issues, there is the fact that metal nitronates are quite inert toward Schiff bases and the aid of a Lewis and/or Brønsted acid is often required.[12] Furthermore, the products of aza-Henry reaction, *β*-nitroamines, are prone to retroaddition.[13] In this work, we present in detail a catalytic asymmetric aza-Henry reaction under phase transfer catalysis (PTC), valid for both nonenolizable and enolizable aldehyde-derived azomethines. Experimental results are complemented with a theoretical investigation of the reaction mechanism, which uncovered a rather unusual hydrogen bonding pattern of the TS of the catalytic reaction with potential implications in a more general context.

Results and Discussion

Background. A recent report[14] from this laboratory has addressed the above issues and found that (Scheme 1) α-amido sulfones,[15] generated from both enolizable and nonenolizable aldehydes, sodium *p*-toluensulfinate, and tert-butyl carbamate, upon reaction with nitromethane in the presence of $CsOH \cdot H_20$ under chiral PTC, provided a good solution to the above problems. Concurrent with our investigations, Herrera and Bernardi have also documented an aza-Henry reaction of similar characteristics.[16] In our study, the initial screen of several cinchone-based quaternary ammonium salts[17] for the reaction of nitromethane with α-amido sulfones, Scheme 1, revealed that *N*-Boc derivatives **1** provide the best results in terms of enantioselectivity. Among the catalysts tested, *N*-benzylquininium chloride **A** was the optimum, a phase transfer catalyst commercially available at relatively low cost.

The exploration of different chiral ammonium salt catalysts of varying skeletal configuration and functionality led to the following conclusions: (a) for production of products of *R* configuration, catalyst **A**, derived from quinine, gives rise to slightly higher selectivities than the cinchonidine-derived counterpart **B**, whereas production of *S* products in high selectivity is conducted by the cinchonine derived salt **C**; (b) blocking the free secondary hydroxyl group of the catalysts in the form of benzyl ether function (catalysts **D** and **E**) drastically disrupts catalytic activity, reaction conversions being typically <10%. This latter observation was interpreted in terms of the key role played by hydrogen bonding interaction during substrate activation. Actually, an intringuing hydrogen-bond network activation pattern, which will be outlined later, has been computationally identified to be the responsible of the observed reactivity and selectivity. In general, for reactions involving nitromethane, Scheme 1, the corresponding adducts **5** were obtained in isolated yields in the 70−80% range and, most remarkably, with very high enantioselectivity, typically 95% *ee*.

Optimization and Scope. Given the observations noted above and owing to the lack of methods for the production of α,*β*-disubstituted *β*-nitroamines of high enantiomeric purity, we decided to explore the validity of the approach for various types of nitroalkanes other than nitromethane. Besides enantioselectivity, control of the relative *syn/anti* configuration of the newly generated stereocenters constitutes an additional difficulty. The initial screening of *N*-protected α-amido sulfones **1a**, **2a**, **3a** and phenyl *N*-phosphinoyl imine **4a**,[18] employing chiral quaternary ammonium salt **A** in the presence of $CsOH \cdot H_2O$, Table 1, revealed the α-amido sulfone **1a** to be the most suitable azomethine precursor for the aza-Henry reaction with nitroethane. Whereas the α-amido sulfones **2a**, **3a** and imine **4a** were poor imine surrogates in terms of reactivity, diastereoselectivity, and/or enantioselectivity (Table 1), α-amido sulfone **1a** provided the desired adduct **6a** in good chemical yield and, most notably, with very high diastereo- and enantioselectivity.

It was also found that solvent influences both reactivity and stereoselectivity (Table 2). For example, the addition of water to the reaction mixture to mimic a more traditional liquid−liquid biphasic system (entries 3 and 6) disrupted not only the reactivity (23 and 30% conversions after 44 h) but, more importantly, also the diastereo- and enantioselectivity (compare entries 3 and 6 with entries 2 and 5). Solvents of increased polarity such as CH_2Cl_2 and THF produced diminished enantiomeric excesses of the corresponding *syn* adducts **6a** and **6b** and had an

(11) For recent examples of enantioselective aza-Henry reaction with aliphatic *N*-Boc imines, see refs 6d and 8f.
(12) Adams, H.; Anderson, J. C.; Peace, S.; Pennell, A. M. K. *J. Org. Chem.* **1998**, *63*, 9932–9934.
(13) (a) Sturgess, M. A.; Yarberry, D. J. *Tetrahedron Lett.* **1993**, *34*, 4743–4746. (b) Anderson, J. C.; Peace, S.; Pih, S. *Synlett* **2000**, 850–852.
(14) Palomo, C.; Oiarbide, M.; Laso, A.; López, R. *J. Am. Chem. Soc.* **2005**, *127*, 17622–17623.
(15) For a review on the preparation and reactivity of α-amidosulfones, see: (a) Petrini, M. *Chem. Rev* **2005**, *105*, 3949–3977. For recent examples involving α-amidosulfones in cinchone catalyzed Mannich reactions, see: (b) Marianacci, O.; Micheletti, G.; Bernardi, L.; Fini, F.; Fochi, M.; Pettersen, D.; Sgarzani, V.; Ricci, A. *Chem.−Eur. J.* **2007**, *13*, 8338–8351. (c) Lou, S.; Dai, P.; Schauss, S. E. *J. Org. Chem.* **2007**, *72*, 9998–10008. (d) Niess, B.; Jørgensen, K. A. *Chem. Commun.* **2007**, 1620–1622. (e) Song, J.; Shih, H.; W; Deng, L *Org. Lett.* **2007**, *9*, 603–606.
(16) Fini, F.; Sgarzani, V.; Pettersen, D.; Herrera, R. P.; Bernardi, L.; Ricci, A. *Angew. Chem., Int. Ed.* **2005**, *44*, 7975–7978.
(17) For cinchone-based quaternary ammonium salts catalyzed reactions, see: (a) Maruoka, K.; Oii, T. *Chem. Rev.* **2003**, *103*, 3013–3028. (b) Oii, T.; Maruoka, K. *Acc. Chem. Res.* **2004**, *37*, 526–533. (c) O'Donell, M. *Acc. Chem. Res.* **2004**, *37*, 606–517. (d) Lygo, B.; Andrews, P. I. *Acc. Chem. Res.* **2004**, *37*, 518–525. For a recent review on the application of phase transfer catalysts, see: (e) Hashimoto, T.; Maruoka, K. *Chem. Rev.* **2007**, *107*, 5656–5682.
(18) The corresponding *N*-phosphinoyl protected α-amido sulfone did not react under the PTC conditions employed. The enantiomeric purities were determined by HPLC.

Table 1. Effect of the Imine Protecting Group (PG) on the Yield and Selectivity of the Aza-Henry Reaction of Nitroethane under PTC[a]

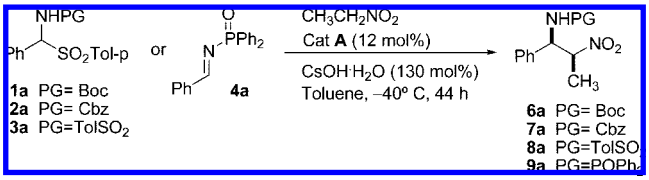

compound	product	conversion (%)	*syn:anti*[b]	*ee* (%)[c]
1a	**6a**	>95	92:8	90
2a	**7a**	20	60:40	67
3a	**8a**	83	50:50	0
4a[d]	**9a**	84	80:20	78

[a] Reactions conducted at 1 mmol scale in dry toluene (3 mL) under a nitrogen atmosphere employing 5 equiv of nitroethane. [b] Determined by ^{1}H NMR and HPLC. [c] Determined by HPLC (see Supporting Information for details). [d] CsOH·H_2O (30 mol %) was employed.

Table 2. Effect of the Solvent in the Aza-Henry Reaction of Nitroethane with *N*-Boc Protected α-Amido Sulfones **1a** and **1b** under PTC[a]

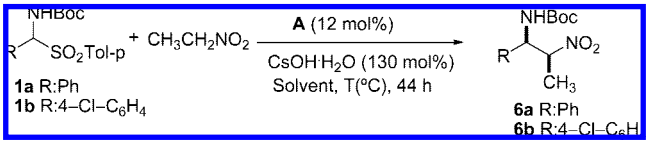

entry	R	solvent	*T* (°C)	conversion (%)	*syn:anti*[d]	*ee* (%)[e]
1	Ph	Toluene	−50	>95	93:7	94[f]
2			−20	>95	89:11	63
3		Toluene + H_2O(50%)	−20[b]	23	50:50	43
4		CH_2Cl_2	−50	40	68:32	78
5	4-Cl−C_6H_6	Toluene	−40[c]	>95	88:12	98[f]
6		Toluene + H_2O(10%)	−40	30	47:53	70 (55 *anti*)
7		CH_2Cl_2	−40	66	55:45	90
8		THF	−40	40	64:34	83

[a] Reactions conducted at 0.5 mmol scale under a nitrogen atmosphere in the indicated solvent (1.5 mL) employing 5 equiv of nitroethane. [b] Reaction carried out at −20 °C to avoid freezing. [c] Below −40 °C, α-amido sulfone **1b** shows limited solubility. [d] Determined by ^{1}H NMR and/or HPLC. [e] Determined by HPLC. [f] The assignment of the absolute and *syn/anti* configuration of adduct **6a** and **6b** was made by comparison with published values (see Supporting Information for details).

important impact in the reactivity and diastereochemical efficiency of the process (entries 4, 7, and 8).

With these insights into the reaction conditions, we next explored the aza-Henry reaction of nitroethane using a range of different *N*-Boc protected α-amido sulfones, Table 3. Both aromatic and aliphatic-substituted α-amido sulfones preferentially produced the *syn*-*β*-nitroamines **6** with variable degrees of diastereoselection[19] and high yield of the *syn:anti* mixture. Electronically diverse aromatic α-amido sulfones (**1a**−**e**, **1g**) displayed excellent enantiomeric excesses (87−98%) for the *syn*-diastereomer. An exception is the 3-nitro substituted α-amido sulfone **1f**, which produced the corresponding *syn*-adduct **6f** with low enantiomeric excess and almost no *syn:anti* selectivity. *Syn* diastereo selection for the rest of aromatic α-amido sulfones ranged from 73:27 (entry 5) to 95:5 ratios (entry 3). Configuration of adducts **6a**−**g** was established by comparison with published values (see Supporting Information).

In general, the enantiomeric excesses obtained in the aza-Henry reaction with nitroethane were slightly higher to those obtained in the reaction with nitromethane (data in parenthesis; entries 1, 2, and 7). The potential of this catalytic approach was further demonstrated by the reaction of nitroethane with enolizable aldehyde-derived α-amido sulfones (**1h**−**l**). As a general trend, the reaction employing alkyl α-amido sulfones produced adducts **6** in good yields and high enantiomeric excess of the corresponding *syn*-adducts (90−96% *ee*). Good *syn* diastereoselectivity was achieved with linear alkyl substituted α-amido sulfones **1h**, **1i**, and **1j** (entries 8, 9, and 10). Nevertheless, reactions involving substrates bearing branched alkyl groups (entries 11, 12) resulted in a considerably attenuated *syn*:*anti* selectivity albeit both the *syn* and the *anti* product were obtained in excellent enantioselectivity.

Due to the essential lack of methods for the production of α,*β*-disubstituted *β*-nitroamines, we decided to explore the validity of the approach for long chain and functionalized nitroalkanes and provide an entry to polifunctional amino compounds. As shown in Table 4, nitroalkanes such as nitropropane, nitropentane, 4-nitropent-1-ene, 2-nitropropane, 1,1-diethoxy-2-nitroethane, 5,5-dimethyl-2-nitromethyl-1,3-dioxane, and ethyl-3-nitropropanoate react with both aromatic and aliphatic-substituted α-amido sulfones to preferentially produce *syn β*-nitroamines. For example, linear nitroalkanes (entries 1−4, 9, and 12) produced adducts **6** in good yields and good *syn* diastereoselectivities; *β*-branched chain nitroalkanes afforded less regular diasteromeric ratios ranging from a good 90:10 ratio (entry 10) to a complete loss of diastereoselection (entry 11). In general, reactions employing alkyl α-amido sulfones produced *syn* adducts in higher enantiomeric excesses (90−99% *ee*) compared to those employing aryl α-amido sulfones (80−95% *ee*). In contrast, the aza-Henry reaction employing an α-branched nitroalkane such as 2-nitropropane displayed a poor enantiomeric excess for adducts **6q** and **6t** (entries 5 and 8).

Chemical Elaboration of Adducts. New Entry to Vinilogous Amino Acids. As outlined in Scheme 2, the *β*-nitroamines obtained in the PTC aza-Henry reaction of α-amido sulfones with nitroalkanes constitute valuable intermediates for the synthesis of a variety of enantioenriched compounds such as α-aminoacids[20] and 1,2-diamines. Even though the elaboration of *β*-nitroamines into 1,2-diamines seems trivial, there is a shortage of methods for the access to enantioenriched dialkyl 1,2-diamines. Thus, the present aza-Henry reaction, that allows the reaction of enolizable aldehyde-derived azomethines with nitroalkanes other than nitromethane, provides a new access to a wide range of 1,2-diamine compounds.

For example, using known procedures, the reduction of the nitro group in **6k** led to the corresponding monoprotected diamine which was converted into the more stable *N*-Boc diprotected diamine **11** (Scheme 3). Also, the simultaneous reduction of the nitro group and deprotection of the *N*-Boc in the *syn*-**6k** (99:1 *syn:anti*, 91% *ee*) afforded in one step the hydrochloric salt **12** in high yield. An additional illustrative example is the transformation of adduct **6x** into compound **13**, which is an orthogonally protected form of 3-aminodeoxystatine, an isosterically modified statine analogue.[21] Configuration of adducts **12** and **13**, and therefore of their immediate precursors

(19) In control experiments, the d.r. values of the reaction of **1a** and **1b** were measured at different degrees of reaction conversion, observing no dependence of the d.r. value with conversion.

(20) See refs 7a and 8c.

Table 3. Aza-Henry Reaction of Nitroethane with Azomethines Generated from α-Amido Sulfones **1** under PTC[a]

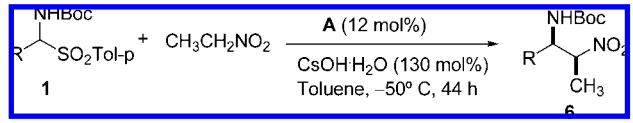

entry	α-amido sulfone	R	product	yield (%)	*syn:anti*[b]	*ee* (%)[c] *syn*
1	**1a**	Ph	**6a**	88 (79)[d]	93:7	94 (91)[d]
2	**1b**[e]	4-Cl−C_6H_4	**6b**	70 (79)[d]	82:18	98 (80)[d]
3	**1c**	4-MeO−C_6H_4	**6c**	87 (82)[d]	95:5	90 (91)[d]
4	**1d**	4-Me−C_6H_4	**6d**	93	92:8	90
5	**1e**	3-Me−C_6H_4	**6e**	98	73:27	87
6	**1f**	3-NO_2−C_6H_4	**6f**	68 (66)[e]	58:42 (75:25)[e]	40 (77)[e]
7	**1g**	2-furyl	**6g**	80 (72)[d]	81:19	95 (84)[d]
8	**1h**	$PhCH_2CH_2$	**6h**	90	90:10	92
9	**1i**	CH_3CH_2	**6i**	90	94:6	>90
10	**1j**	$(CH_3)_2CHCH_2$	**6j**	85	97:35	96
11	**1k**	$(CH_3)_2CH$	**6k**	90	67:33	92 (≥95 *anti*)
12	**1l**	cC_6H_{11}	**6l**	65	60:40	95 (97 *anti*)

[a] Reactions conducted at 0.5 mmol scale in dry toluene (1.5 mL) under a nitrogen atmosphere employing 5 equiv of nitroethane. [b] Determined by ^{1}H NMR and/or HPLC. [c] Determined by HPLC (see Supporting Information for details). [d] In parenthesis are data for the aza-Henry reaction with nitromethane. [e] Reaction conducted at −40 °C.

Table 4. Scope of the Aza-Henry Reaction with Azomethines Generated from α-Amido Sulfones **1** under PTC[a]

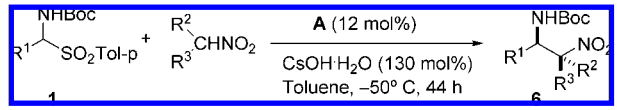

entry	1	R^1	R^2	R^3	prod.	yield (%)	*syn:anti*[b]	*ee*(%)[c] *syn*
1	**1a**	Ph	H	CH_3CH_2	**6m**	88	91:9	94
2	**1c**	4–MeO–C_6H_6	H	CH_3CH_2	**6n**	77	89:11	80
3			H	$CH_3(CH_2)_3$	**6o**	82	89:11	83
4			H	CH_2=$CH(CH_2)_2$	**6p**	80	76:24	95
5	**1d**	4–Me–C_6H_6	CH_3	CH_3	**6q**	52	--	20
6	**1g**	2–furyl	II	$(EtO)_2CII$	**6r**	56	75:25	85
7	**1h**	$PhCH_2CH_2$	H	$(EtO)_2CH$	**6s**	66	67:33	96
8			CH_3	CH_3	**6t**	75	--	30
9	**1j**	$(CH_3)_2CHCH_2$	H	CH_3CH_2	**6u**	91	93:7	97
10			H	$(EtO)_2CH$	**6v**	70[d]	90:10	99
11			H	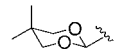	**6w**	63[c]	55:45	≥90
12			H	EtO_2CCH_2	**6x**	70	75:25	97

[a] Reactions conducted at 0.5 mmol scale in dry toluene (1.5 mL) under a nitrogen atmosphere employing 5 equiv of the corresponding nitroalkane. [b] Determined by ^{1}H-NMR and/or HPLC. [c] For *syn* adduct; determined by HPLC (see Supporting Information for details). [d] Reaction performed at 5 mmol scale. [e] Reaction conducted at −40° C.

Scheme 2. Useful Synthetic Transformations of β-Nitroamines

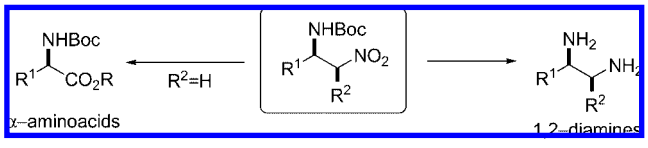

6k and **6x**, was determined by comparison of chiroptic and chromatographic data with published values.[22,23] For the remaining *syn* aza-Henry adducts **6m**−**w**, it was assumed on the basis of an uniform reaction mechanism.

To expand the synthetic utility of the present method, we decided to investigate other, little explored, applications of the functionalized nitroamine adducts. In particular, it is known that nitro groups positioned β to an electron-withdrawing group can be eliminated and give alkenes on treatment with base.[24] Actually, when adduct **6x** (mixture *syn:anti* 75:25) was treated with 1,8-diazabicyclo[5.4.0]undec-7-ene (DBU) at room temperature, the γ-amino α,β-unsaturated ester **14x** was, to our delight, cleanly produced in high yield and excellent enantioselectivity (Scheme 4a).[25] On the other hand, prior chromatographic separation of *anti*-**6x** from the *syn*/*anti* mixture and subsequent treatment with DBU afforded the same compound

(21) For references on the topic, see: (a) Babine, R. E.; Bender, S. L. *Chem. Rev.* **1997**, *97*, 1359–1472. (b) Richards, A. D.; Roberts, R.; Dunn, B. M.; Graves, M. *Kay. J. FEBS. Lett.* **1989**, *247*, 113–117. (c) Maly, D. J.; Huang, L.; Ellman, J. A. *ChemBioChem* **2002**, *3*, 16–37.

Scheme 3. Transformation of Aza-Henry Compounds into 1,2-Diamines

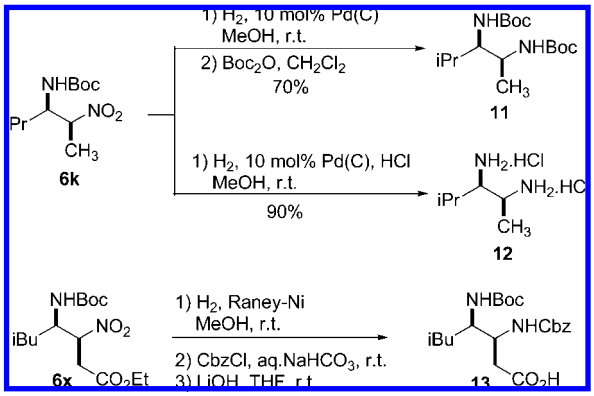

Scheme 4. Base-Promoted Synthesis of γ-Amino α,β-Unsaturated Ester **14x**

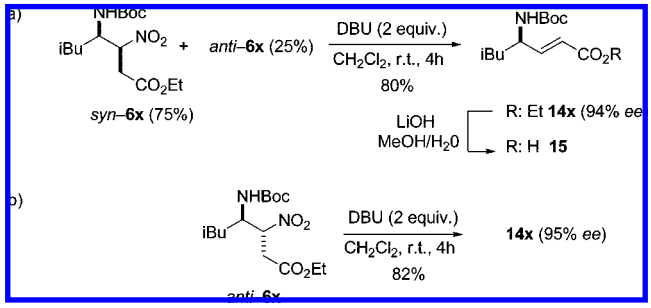

Scheme 5. Formal Catalytic Enantioselective 2-Ethoxycarbonylvinylation of *N*-Acylimines

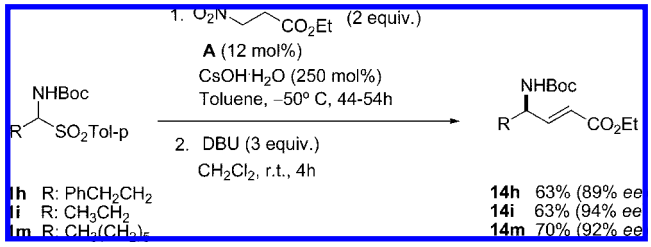

14x, from which the configuration of the *anti*-**6x** adduct could be inferred to be (*R*, *R*) (Scheme 4b). This assumption would indicate that the present catalytic aza-Henry reaction proceeds with almost perfect π-face selectivity over the azomethine compound.

Generalization of the base-promoted nitrous acid elimination process was successful for other nitroamine adducts **14h**, **i**, **m** (Scheme 5). Hence, this process represents an unprecedent entry to highly enantiopure vinylogous amino acids,[26] which are effective modulators of secondary and tertiary structure in polypeptide chains,[27] constituents of important naturally occurring molecules[28] and versatile intermediates of structurally and biologically relevant compounds.[29] It is important to notice that the overall process, shown in Scheme 5, represents an olefin umpolung strategy[30] carried out in this case, under catalytic conditions[31] and with good overall yield and selectivity.

Reaction Mechanism

The present aza-Henry reaction proceeds under non homogeneous reaction conditions and involves a concatenated sequence of steps which turn the full understanding of the reaction mechanism challenging. Despite this complexity, the combination of some experimental observations with performed

(22) Due to some discrepancy in the absolute value of the optical rotation, relative configuration was confirmed by X-ray crystal structural analysis of adduct **6x**.

(23) For adduct **12**, see: (a) Merino, P.; Lanaspa, A.; Merchan, F. L.; Tejero, T. *Tetrahedron: Asymmetry* **1997**, *8*, 2381–2401. For adduct **13**, see: (b) Arrowsmith, R.; Carter, K.; Dann, J. G.; Davies, D. E.; Harris, J.; Morton, J. A.; Lister, P.; Robinson, J. A.; Williams, D. *J. Chem. Soc., Chem. Commun.* **1986**, 755–757.

(24) Ono, N. *The Nitro Group in Organic Synthesis*; Wiley-VCH: New York, 2001; pp 218−230.

(25) Transformation of **14x** into the corresponding knownγ-aminoα,β-unsaturated acid **15** allowed the determination of the absolute configuration (see Supporting Information). The enantiomeric purity was determined by HPLC.

(26) Access to these interesting compounds has traditionally relied on the olefination of α-amino aldehydes. See, for instance: (a) Gryko, D.; Chalko, J.; Jurczak, J. *Chirality* **2003**, *15*, 514–541. (b) Reetz, M. T *Chem. Rev.* **1999**, *99*, 1121–1162. Also, see: (c) Kotkar, S. P.; Chavan, V. B.; Sudalai, A. *Org. Lett.* **2007**, *9*, 1001–1004.

(27) For recent examples, see: (a) Bang, J. K.; Naka, H.; Teruya, K.; Aimoto, S.; Konno, H.; Nosaka, K.; Tatsumi, T.; Akaji, K. *J. Org. Chem.* **2005**, *70*, 10596–10599. (b) Grison, C.; Coutrot, P.; Geneve, S.; Didierjean, C.; Marraud, M. *J. Org. Chem.* **2005**, *70*, 10753–10764. (c) Baldauf, C.; Günther, R.; Hofmann, H.-J. *Helv. Chim. Acta* **2003**, *86*, 2573–2588.

(28) (a) Fusetani, N.; Matsunaga, S.; Matsumoto, H.; Takebayashi, Y. *J. Am. Chem. Soc.* **1990**, *112*, 7053–7054. (b) Coleman, J. E.; Dilip de Silva, E.; Kong, F.; Andersen, R. J. *Tetrahedron* **1995**, *51*, 10653–10662. (c) Wolin, R. L.; Santillán, A, Jr.; Barclay, T.; Tang, L.; Venkatesan, H.; Wilson, S.; Lee, D. H.; Lovenberg, T. W *Bioorg. Med. Chem.* **2004**, *12*, 4493–4509. (d) Swarna, V. M.; Undem, B. J.; Korlipara, V. L. *Bioorg. Med. Chem.* **2007**, *17*, 890–894.

(29) Peptide isosters: (a) Thoen, J. C.; Morales-Ramos, A. I.; Lipton, M. A. *Org. Lett.* **2002**, *4*, 4455–4458. (b) Palomo, C.; Oiarbide, M.; Landa, A.; Esnal., E.; Linden, A. *J. Org. Chem.* **2001**, *66*, 4180–4186. (c) Broady, S. D.; Rexhausen, J. E.; Thomas, E. J. *J. Chem. Soc., Perkin Trans.* **1999**, *1*, 1083–1094. Iminosugars: (d) Hulme, A. N.; Montgomery, C. H *Tetrahedron Lett.* **2003**, *44*, 7649–7653. Glutamate receptors: (e) Oba, M.; Koguchi, S.; Nishiyama, K. *Tetrahedron* **2002**, *58*, 9359–9363. (f) Daunan, P.; Saint-Fuscien, C. D.; Acher, F.; Prèzeau, L.; Brabet, I.; Pin, J.; Dodd, R. H. *Bioorg. Med. Chem. Lett.* **2000**, *10*, 129–133. (g) Dauban, P.; Saint-Fuscien, C. D.; Dodd, R. H. *Tetrahedron* **1999**, *55*, 7589–7600. Amino acids: (h) Hayashi, T.; Yamamoto, A.; Ito, Y.; Nishioka, E.; Miura, H.; Yanagi, K. *J. Am. Chem. Soc.* **1989**, *111*, 6301–6311. (i) Jumnah, R.; Williams, J. M. J.; Williams, A. C. *Tetrahedron Lett.* **1993**, *34*, 6619–6622. (j) Bower, J. F.; Jumnah, R.; Williams, A. C.; Williams, J. M. J. *J. Chem. Soc., Perkin Trans. 1* **1997**, 1411–1420. (k) Burgess, K.; Liu, L. T.; Pal, B *J. Org. Chem.* **1993**, *58*, 4758–4763. Alkaloids: (l) Magnus, P.; Lacour, J.; Coldham, I.; Mugragr, B.; Bauta, W. B. *Tetrahedron* **1995**, *51*, 11087–11110. (m) Trost, B. M. *Angew Chem., Int. Ed. Engl.* **1989**, *28*, 1173–1094. Carbohydrate derivatives: (n) Trost, B. M.; Van Vranken, D. L. *J. Am. Chem. Soc.* **1993**, *115*, 444–458.

(30) For reviews on the topic, see: (a) Seebach, D. *Angew. Chem., Int. Ed. Engl.* **1969**, *8*, 639–649. (b) *Umpoled Synthons*; Hase, T. A., Ed.; John Wiley: New York, 1987.

(31) To the best of our knowledge, base-promoted elimination of nitrous acid to afford alkenes has only been employed in combination with racemic transformations: Michael addition to ethyl β-nitroacrylate: (a) Patterson, J. W.; McMurry, J. E. *Chem. Commun.* **1971**, 488–489. Henry and Michael reactions of nitroalkanes: (b) Seebach, D.; Hoekstra, M. S.; Protschuck, G. *Angew. Chem., Int. Ed.* **1977**, *16*, 321–322. (c) Mori, K.; Kitahara, T. *Tetrahedron* **1984**, *40*, 2935–2944. (d) Ballini, R.; Fiorini, D.; Palmieri, A. *Tetrahedron. Lett.* **2004**, *45*, 7027–7029. (e) Bakuzis, P.; Bakuzis, M. L. F.; Weingartner, T. F. *Tetrahedron Lett.* **1978**, *19*, 2371–2374. (f) Ballini, R; Bosica, G. *Tetrahedron* **1995**, *51*, 4213–4222. Alkylation of nitroesters: (g) Seebach, D.; Henning, R.; Mukhopadhyay, T *Chem. Ber.* **1982**, *115*, 1705–1720. Diels-Alder reactions: (h) Danishesfsky, S.; Prisbylla, M. P.; Hiner, S. *J. Am. Chem. Soc.* **1978**, *100*, 2918–2920.

(32) For related proposals involving catalytic PTC reaction conditions, see: Mannich reaction: ref 15b; Strecker reaction: Herrera, R. P.; Sgarnazi, V.; Bernadi, L.; Fini, F.; Pettersen, D.; Ricci, A. *J. Org. Chem.* **2006**, *71*, 9869–9872.

Scheme 6. Enantioselective Aza-Henry Reaction between Nitromethane and (a) α-Amido Sulfone, under PTC Conditions, and (b) Preformed *N*-Acyl Imine

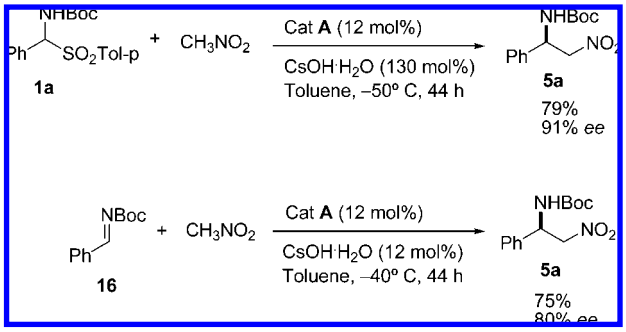

quantum calculations allowed us to propose a general reaction scheme wherein the role played by the reactants, the added base, and the catalyst, as well as a plausible stereochemical model for the transfer of chirality, can be identified as described below.

Experimental Observations. A primary observation was that the reaction outcome is essentially identical, as shown in Scheme 6, whether we started from the α-amido sulfone **1a** or the corresponding preformed *N*-acyl imine **16**. Accordingly, imine formation from the respective α-amido sulfones apparently takes place in an independent event that precedes the aza-Henry reaction and the evolving sulfinate salts have not influence in the latter process. On the other hand, NMR monitoring of the reaction mixture of **1a** at different degrees of reaction conversion revealed no peaks corresponding to the *N*-acyl imine intermediate. The absence of appreciable amounts of *N*-acyl imine intermediate along the course of the reaction appears to indicate that base-promoted generation of imine proceeds slower than the subsequent imine consumption via carbon−carbon coupling (aza-Henry reaction).

A third experimentally supported important conclusion is that the OH^- anions present in the reaction mixture are not by their own the responsible of imines formation from α-amido sulfone precursors. Instead, the base-promoted conversion of starting α-amido sulfones into the *N*-acyl imines can be ascribed to an organic base generated in the environment, most likely nitronate anion, based on the following two observations: (1) treatment of α-amido sulfone **1a** with 1.3 equiv of CsOH in the presence of ammonium salt **A** (12 mol%) in toluene as solvent at −50 °C for as long as 44 h did not produce any appreciable reaction, and starting **1a** was recovered unaltered; (2) neither reaction was observed when **1a** was treated with CsOH (1.3 equiv) and nitroethane in toluene at −50 °C in the absence of catalyst **A**. So, both nitroalkane and catalyst **A** are required for imine generation. We postulate the general reaction scheme represented in Figure 2.[32] Thus, the initially originated nitronate anion will be the actual base that promotes elimination of sulfinic acid from α-amido sulfones to render the intermediate *N*-acyl imines. Direct implication of nitronate anion in imine formation is further sustained by the fact that when more acidic nitroalkanes such as methyl 2-nitroacetate are involved, the aza-Henry reaction takes place sluggishly (15% conversion after 44 h). This slowness could be ascribed to the lower basicity of the corresponding nitronate anion in this particular case. Steric effects, which could be invoked as the source of the lower reactivity of methyl 2-nitroacetate, are ruled out since 2-nitropropane, which bears similar steric congestion, but displays lower acidity, gave the aza-Henry reaction satisfactorily (>95% conversion after 44 h). In addition, it was observed that the

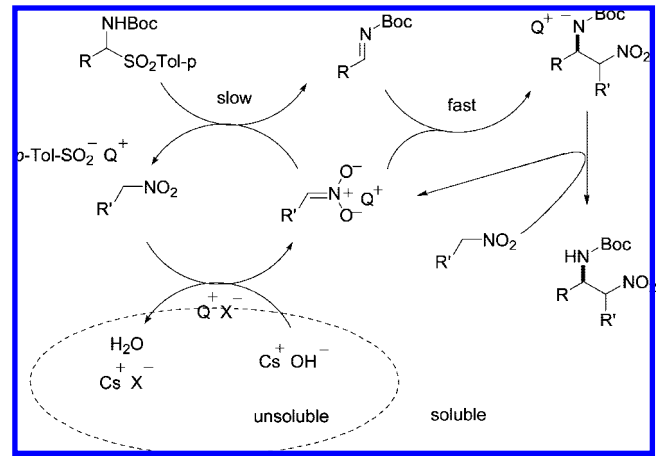

Figure 2. General scheme for the aza-Henry reaction involving α-amido sulfones under PTC conditions.

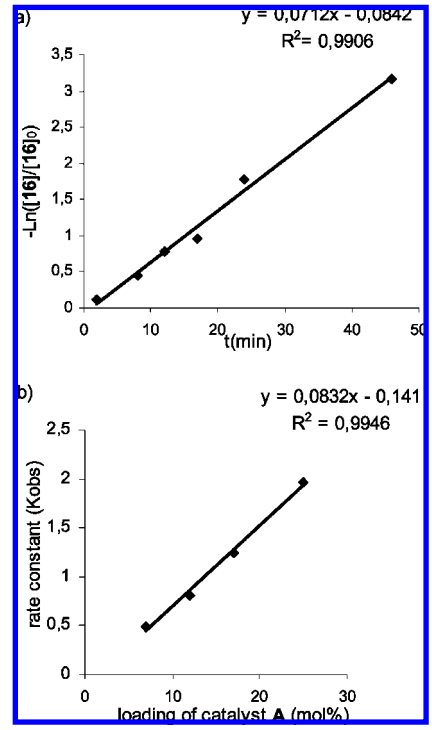

Figure 3. Kinetic studies on the aza-Henry reaction of **16** with nitromethane under (a) pseudoconstant concentration of nitromethane and (b) variable loading of catalyst **A**.

outcome of the aza-Henry reaction is independent of the excess amount of CsOH employed, which secures high reproducibility irrespective of the amount of inorganic salt added.

Kinetic Studies. To obtain further information about the reaction mechanism, we carried out kinetic studies on the aza-Henry reaction. The parameters of the reaction between imine **16** and nitromethane catalyzed by **A** were determined by monitoring the consumption of phenyl *N*-Boc imine **16** by ^{1}H NMR. In the first set of experiments (Figure 3a), the reaction order in phenyl *N*-Boc imine **16** was established by using a large excess of nitromethane (15 equiv) and 12 mol % of catalyst. Plotting in $-\ln([\mathbf{16}]/[\mathbf{16}_0])$ versus time gave a straight line ($R^2 = 0.9906$), which indicates first-order dependence in the imine. The reaction order in catalyst **A** was established by

determining the kinetic rate constants (k_{obs}) at various catalyst concentrations (7, 12, 18, and 25 mol %). Plotting of k_{obs} versus the catalyst loading gave also a straight line for *N*-benzylquininium chloride **A** ($R^2 = 0.9946$, Figure 3b), indicating the first-order dependence in catalyst. Unfortunately, the reaction order in nitromethane could not be determined using this methodology due to experimental constraints such as the relatively high volatility of nitromethane and the low solubility of the reaction product in the reaction media which difficulted the measurement of the actual consumption of nitromethane (or actual formation of coupling product).[33] However, for the subsequent quantum calculations, we assumed that the C−C coupling step in the aza-Henry reaction is unimolecular with respect to each reactant (imine and nitrocompound) and catalysts.

Given the above results, the next questions that we addressed were to establish the role of the free hydroxyl group of catalyst **A** for reaction activity and the origin of the high π-facial selectivity with the present catalytic system. For example, we have experimentally shown that the free hydroxyl group in the catalyst **A** plays a key role in substrate activation because the corresponding *O*-benzylated derivatives **D** and **E** displayed a significant lower catalytic activity (typical conversions under 10%) in the reaction with nitromethane. These results suggest that the catalyst exhibits dual functions and that the free OH group participates in the activation of one or both substrates by hydrogen bonding (H−B). The fact that the addition of nitromethane to *N*-Boc imine under phase transfer conditions produced a similar result to that obtained starting from the corresponding α-amido sulfone, Scheme 6, aimed us to study computationally the reaction involving already formed imine. Our first goal was to understand the structure of the possible hydrogen-bonded reactant complexes and the participation of the OH during the transition state of the reaction.

Computational Methods. For the initial model studies, all structures were optimized using the functional B3LYP[34] and the 6-31G* basis sets as implemented in Gaussian 03.[35] All energy minima and transition structures were characterized by frequency analysis. The energies reported in this work include zero-point vibrational energy corrections (ZPVE) and are not scaled. The stationary points were characterized by frequency calculations to verify that they have the right number of negative eigenvalues. The intrinsic reaction coordinates (IRC)[36] were followed to verify the energy profiles connecting each TS to the correct associated local minima. Charge transfers and atomic charges were calculated within the natural bond orbital (NBO) analysis.[37] For the enantioselectivity studies, a preliminary search was conducted with the D95V basis set and the most favored structures were reoptimized at B3LYP/6-31G* level. Single point calculations were performed at a higher B3LYP/6-311++G**//B3LYP/6-31G* level to obtain more accurate energies of the most relevant structures. The single-point calculations with the self-consistent reaction field (SCRF) based on the IEF-PCM[38] solvation model (toluene $\epsilon = 2.378$) were carried out at B3LYP/6-311++G** level on the previously optimized structures.

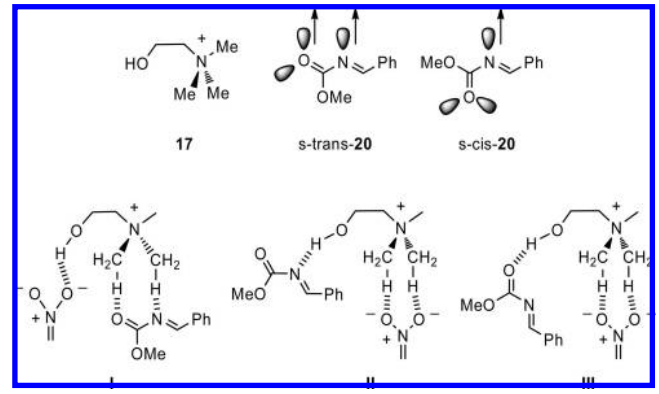

Figure 4. Representation of computational models **17** and **20**, and three possible ternary complexes, showing distinct hydrogen bond networks.

Coordination of the Reactants with the Catalyst. Model Studies. We set out to study computationally the mode by which the catalyst and the reacting nitro compound and *N*-acyl imine substrates interact (Figures 4 and 5). For optimizing computational time, the rather large catalyst molecule **A** was substituted with the hydroxyethyl trimethyl ammonium cation **17**, which bears the OH and the $^{+}$NCH groups linked by an ethylene spacer. This minimal catalyst model comprises the most salient structural elements of the real catalyst **A**. On the other hand, among the reactant nitro compounds, both nitromethane **18** and its deprotonated form **19** were considered, whereas *N*-methoxycarbonyl imine **20** was selected as the iminic component instead of the larger tert-butoxycarbonyl analog. From a preliminary examination of the structures of these four molecular entities **17**−**20**, several features can be inferred: (1) catalyst **A** and its model **17** show two sites with high H-bonding donor ability, an O−H and a $^{+}$N−C−H site;[39] (2) Both nitroalkanes and their conjugate bases (nitronates) bear strongly coordinating N−O^{-} groups; (3) *N*-acyl imines can act as Lewis bases through either the N or the carbonyl O atom; (4) *N*-acyl imines can exist in either s-cis (cisoid) or s-trans (transoid) conformations. We first addressed the conformational issue. Although both s-trans and s-cis conformations bear similar energies in the isolated form, the complexation with a multiple hydrogen bond donor like **A** or model **17** appears to fit better in the s-trans form, which has two H-bond acceptor atoms (O, N) pointing toward the same site (Figure 4); conversely, the O and N atoms of the s-cis form point in opposite directions and their simultaneous coordination to a local multiple H-bond donor site seems less effective. In fact, the calculated energy for the **17**:**20** complex is about 3.6 kcal/mol lower for the s-trans conformer (see Supporting Information for full data). Accordingly, only s-trans conformations were considered in the subsequent studies. On the basis of the aforementioned structural features, several

(33) Substrate solubility constraints were found during kinetic studies of a thiourea-catalyzed Michael reaction to unsaturated imides. See: (a) Inokuma, T.; Hoashi, Y.; Takemoto, Y. *J. Am. Chem. Soc.* **2006**, *128*, 9413–9419.

(34) (a) Lee, C.; Yang, W.; Parr, R. G. *Phys. Rev. B* **1988**, *37*, 785–789. (b) Becke, A. D. *J. Chem. Phys.* **1993**, *98*, 5648–5652. (c) Kohn, W.; Becke, A. D.; Parr, R. G. *J. Phys. Chem.* **1996**, *100*, 12974–12980.

(35) Frisch, M. J.; *Gaussian 03*, revision D.03; Gaussian, Inc.: Wallingford, CT, 2004.

(36) Gonzalez, C.; Schlegel, H. B. *J. Phys. Chem.* **1990**, *94*, 5523–5527.

(37) (a) Reed, A. E.; Weinstock, R. B.; Weinhold, F. *J. Chem. Phys.* **1985**, *83*, 735–746. (b) Reed, A. E.; Curtiss, L. A.; Weinhold, F. *Chem. Rev.* **1988**, *88*, 899–926.

(38) (a) Cancès, E.; Mennucci, B.; Tomasi, J. *J. Chem. Phys.* **1997**, *107*, 3032–3047. (b) Cossi, M.; Barone, V.; Mennuci, B.; Tomasi, J. *Chem. Phys. Lett.* **1998**, *286*, 253–260. (c) Tomasi, J.; Mennucci, B.; Cancès, E. J. *Mol. Struct. (Theochem)* **1999**, *464*, 211–226.

(39) Me_3N^{+}−CH···O=C hydrogen bonds have been reported to be the strongest hydrogen bonds of the type C−H···O=C known to date: Cannizaro, C. E.; Houk, K. N. *J. Am. Chem. Soc.* **2002**, *124*, 7163–7169.

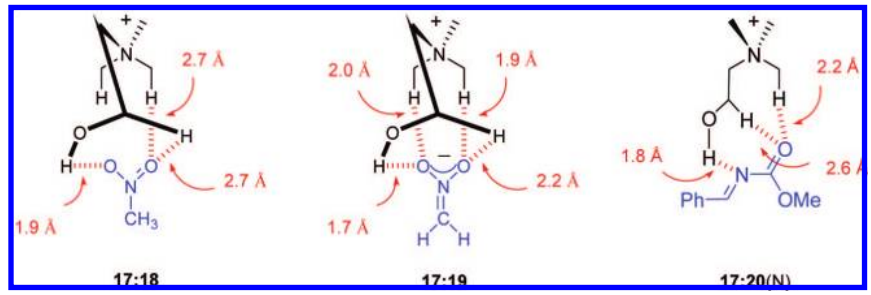

Figure 5. Geometries of the hydrogen bonding complexes **17:18**, **17:19**, and **17:20**(N).

Scheme 7. Hydrogen Bonding Complexes between **17** or Tetramethylammonium Cation (**21**) and the Different Substrates

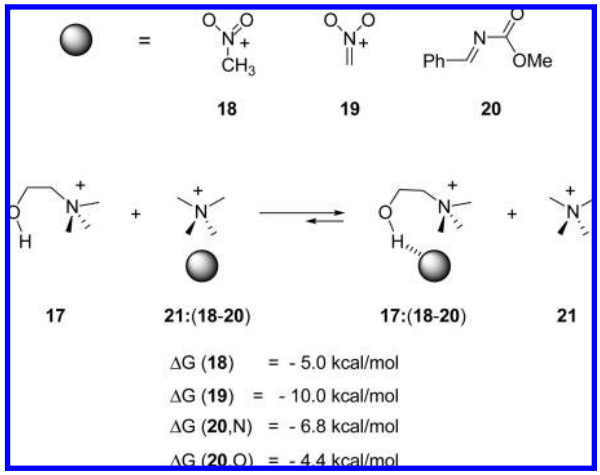

competitive H-bonding patterns[40] can be conceived as representations of the complexes formed among the catalyst and the two components of the reaction, three of which are shown in Figure 4 as simplified models **I**, **II**, and **III**. Although the straightforward comparison of the stability of ternary complexes **I**-**III** (Figure 4) would be a plausible starting point of the study, attempts to do so are met with failure. Several nondesired interactions arising from the flexibility of model **17** and from the presence of polar substituents in both reactants and in **17** led to a high conformational ambiguity and many disperse minima were located, making very difficult the direct evaluation of their binding affinities (see Supporting Information for details and structures).

Accordingly, we carried out alternative calculations aimed at estimating the relative binding energy of the catalyst O−H to either of the reacting species. As shown in Scheme 7, the relative binding energies of complexes **17:18**, **17:19**, **17:20** (N), and **17:20** (O) were computed by comparison of the preferential complexation of the different substrates (nitromethane (**18**), nitronate anion (**19**), and imine (**20**)) to the hydroxylated tetramethylammonium cation (**17**) or tetramethylammonium cation (**21**). For substrate **20**, two distinct complexes were considered: one with N as the coordinating atom **20** (N) and a second one with the carbonyl O as the coordinating atom **20** (O). The computed Gibbs energy variations for the four equilibria were all negative, indicating that the four reactants

Table 5. Charge Distribution and H−B Distances of the Ternary Complexes, Transition States, and Final Adducts, Computed at B3LYP/6-31G*

	electrostatic charge (e^-)[a]			total charge (e^-)[b]		distance (Å)	
stationary point	O (NO_2)	N (imine)	O (imine)	**19**	**20**	OH···X	$N^+CH\cdots O$
17:18	−0.38	−	−	+0.05	−	1.89[c]	−
17:19	−0.64	−	−	−0.80	−	1.67[c]	−
17:20(N)	−	−0.55	−0.70	−	+0.06	1.81[d]	−
$\mathbf{TS_I}$	−0.53	−0.64	−0.70	−0.48	−0.38	1.76[c]	2.23[f]
$\mathbf{TS_{II}}$	−0.53	−0.66	−0.66	−0.54	−0.30	1.82[d]	2.14[g]
$\mathbf{TS_{III}}$	−0.54	−0.63	−0.73	−0.57	−0.30	1.81[e]	2.04[g]
$\mathbf{F_I}$	−0.40	−0.78	−0.78	−0.04	−0.83	1.96[c]	2.09[f]
$\mathbf{F_{II}}$	−0.39	−0.81	−0.77	−0.04	−0.80	1.85[d]	2.60[g]
$\mathbf{F_{III}}$	−0.40	−0.75	−0.81	−0.05	−0.81	1.69[e]	2.36[g]

[a] Charge of the corresponding atom. [b] Total charge of the nitronate fragment (**19**) or the imine fragment (**20**) of the structure. [c] X = O (nitro). [d] X = N (imine). [e] X = O (imine). [f] Refers to the shortest $N^+CH\cdots O{=}C$ bond. [g] Refers to the shortest $N^+CH\cdots O_2N$ bond.

18−**20** bind stronger to the hydroxylated cation **17** than to **21**. Thus, the relative magnitude of ΔG at equilibrium can be taken as a measure of the relative strength of the hydrogen bond in each complex. We found that the hydrogen bonding stabilization energy is maximal for the nitronate **19** (**17:19**, 10.0 kcal/mol) and the preferred binding site of imine **20** is the nitrogen atom (6.8 kcal/mol) vs the oxygen atom (4.4 kcal/mol). From these data, it can be inferred that type **I** ternary complex (Figure 4) is formed preferentially over types **II** or **III** prior to reaction. In addition, deprotonation of nitromethane by the pertinent base in the presence of the catalyst's OH is greatly favored as a much stronger hydrogen bond is formed with nitronate **19** than with neutral nitromethane **18** (5.0 kcal/mol binding energy difference). This differential behavior of nitromethane and its nitronate anion is in agreement with the computed negative charge that develops on the two oxygens upon deprotonation, which markedly increases from −0.38e in nitromethane (**17:18**) to −0.64e in nitronate (**17:19**) (Table 5).

The significant differences of the computed H−B distances are consistent with the above statements (Figure 5). For instance, the $O{-}H\cdots O_2N$ bond length is larger in **17:18** (1.9 Å) than in **17:19** (1.7 Å), and the $N^+CH\cdots O_2N$ interactions are also stronger in nitronate complex **17:19** (1.9 Å, 2.0 Å)[41] than in **17:18** (2.7 Å, 2.7 Å). The bonding distances of the corresponding H−B detected in complex **17:20** (N) (Figure 4) are shorter than those of complex **17:18** but longer than those of **17:19**. These data indicate that imine **17:20** (N) is complexed to the catalyst stronger than nitromethane does but weaker than nitronate does.

Calculations were also carried out introducing the solvent effects, but the results for the four equilibria depicted in Scheme

(40) For previous theoretical studies dealing with organocatalytic reactions where the catalyst exhibits two competitive H-bond donor sites, see: (a) Hamza, A.; Schubert, G.; Soós, T.; Papai, I. *J. Am. Chem. Soc.* **2006**, *128*, 13151–13160. (b) Hammar, P.; Marcelli, T.; Hiemstra, H.; Himo, F. *Adv. Synth. Catal.* **2007**, *349*, 2537–2548.

(41) This findings are in agreement with the reported data about the strength of hydrogen bonds of the type $Me_3N^+{-}CH\cdots O{=}C$, see ref 39.

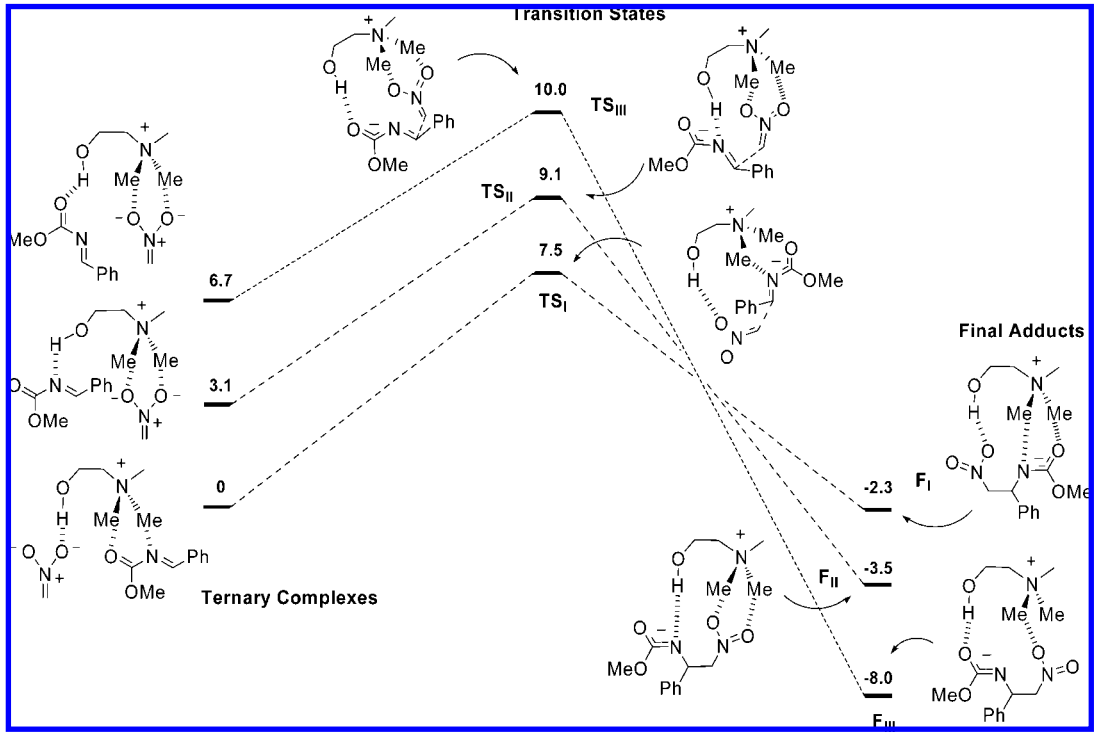

Figure 6. Energy diagram for the three computed pathways ($\mathbf{TS_I}$, $\mathbf{TS_{II}}$, and $\mathbf{TS_{III}}$) in the aza-Henry reaction. Values correspond to free Gibbs energies and are given in kcal/mol.

7 were similar to those obtained in the gas phase. The fact that all computed species have similar electrostatic character may help to cancel the destabilizing effects of the charges at both sides of the equilibrium in the gas phase.

Reaction Transition States. Transition states were computed for the three different reaction models, **I**, **II**, and **III** as shown in Figure 6. $\mathbf{TS_I}$ is the lowest in energy, whereas $\mathbf{TS_{II}}$ and $\mathbf{TS_{III}}$ are 1.6 and 2.5 kcal/mol above in energy, respectively, which correspond to a reaction rate difference of ca. 15-fold slower for $\mathbf{TS_{II}}$ and ca. 100-fold slower for $\mathbf{TS_{III}}$. Thus, as happens in the starting ternary complexes, the most stable TS is that with the catalyst's OH group linked to the nitro group, and the imine component linked through H-bond to the $^{+}$NCH site of the catalyst. The prevalence of this H-bond sequence over other possible sequences is also in agreement with the electronic charge distribution in the TS. Natural population analysis (Table 5) shows that the formation of the C−C bond is accompanied by a charge transfer from the nucleophile to the electrophile, although this transfer is not enough to remarkably weaken the interaction between the OH and NO_2 groups in TS. Monitoring of net electrostatic charge on the oxygen atoms of the NO_2 group when moving from the initial complex **I** to $\mathbf{TS_I}$ and final adduct $\mathbf{F_I}$ shows that most of the intial charge (−0.64e) is retained in TS (−0.53e). With respect to the charge evolution on the N atom of the imine compound, it goes from −0.55e in the complexed imine to −0.66e in $\mathbf{TS_I}$. In addition, due to the early character of $\mathbf{TS_{II}}$ and $\mathbf{TS_{III}}$,[42] the amount of net charge transfer is smaller in $\mathbf{TS_{II}}$ (0.26e) and $\mathbf{TS_{III}}$ (0.23e) than in $\mathbf{TS_I}$ (0.32e). The overall view is that the transition structures and their binding affinities resemble those of the initial ternary complexes rather than the final adducts (Figure 6).

Final Adducts. The most stable complex corresponds to $\mathbf{F_{III}}$ (Figure 6), which shows the catalyst's OH bonded to the carbamate oxygen. On the other hand, charge transfer from the nitronate to the imine is essentially completed (ca. 0.80e), thus the carbamate oxygen in adducts bears most of the negative charge (−0.81e in $\mathbf{F_{III}}$) and the charge in NO_2 oxygen atoms reduces back to the standards of neutral nitroalkane (−0.40e). In $\mathbf{F_I}$, the OH···O_2N bond is much weaker (1.96 Å) than the OH···O_{imine} bond in $\mathbf{F_{III}}$ (1.69 Å), which is at its maximum strength. The energy difference between $\mathbf{F_I}$ and $\mathbf{F_{III}}$ is very large, 5.7 kcal/mol in favor of $\mathbf{F_I}$ (5.7 kcal/mol also in toluene). Nonetheless, this preference may represent a further advantage for the catalyst turnover and for the completion of the reaction, because upon protonation of the carbamate, the weak interaction between neutral NO_2 group and catalyst's OH group would facilitate the final decomplexation of the adduct or its displacement by a new molecule of incoming nitromethane. Later on, solvent effects were introduced and computation of the transition states carried out once again. However, no significant change was obtained with $\mathbf{TS_I}$ being the most favorable and $\mathbf{TS_{III}}$ the less favorable ($\Delta\Delta G^{\ddagger} = 2.5$ kcal/mol).

Enantioselectivity. The next issue to be addressed was the origin of the enantioselectivity of the process. For this purpose, the results from the model study represented in Figure 6, which involves TS geometries $\mathbf{TS_I}$, $\mathbf{TS_{II}}$, and $\mathbf{TS_{III}}$, were considered as starting point with two modifications: now the full chiral catalyst **A**, instead of the model **17**, and *N*-Boc imine[43] **16** were considered as the intervening components. For each sort of transition states, the search of the most favorable conformations of the catalyst **A** was taken, from which four main arrangements

(42) Forming bond C−C distances, **TSI**: 2.18Å; **TSII**: 2.33Å; **TSIII**: 2.39Å.

(43) Because *N*-Boc imines show some preference for s-cis/cisoid conformation in the ground state, TS involving *N*-Boc imines with the O=C−N=C system in their s-cis conformation were also calculated. However, the latter lie around 5 kcal/mol higher in energy than the corresponding s-trans TS, very likely due to the steric interference between the *t*-butyl and the catalyst bicyclic skeleton in the TS. See Supporting Information for more details.

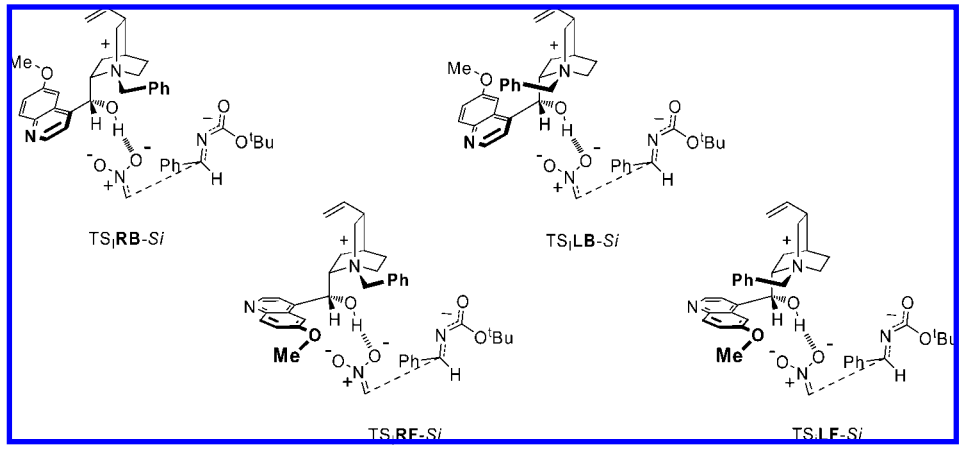

Figure 7. Representation of the transition state geometries corresponding to the attack of nitromethane to the *Si* face of the imine (according to a **TS$_I$** type process). Secondary hydrogen bonds between imine and N^+CH hydrogens have been omitted for clarity.

Table 6. Transition State Energies and Relative Contribution Percentages of the **TS$_I$** Structures at Different Computational Levels

entry	TS	$\Delta\Delta E^{\ddagger a}$		$\Delta\Delta G^{\ddagger a}$		6-311++G** ($\Delta\Delta E^{\ddagger}$)^b		PCM (toluene)^c	
1	TS$_I$**RF**-*Si*	0^d (0)^e	94.9%^{f}	0^d	84.3%^{f}	0^d	92.9%^{f}	0^d	91.5%^{f}
2	TS$_I$**RB**-*Si*	2.5 (2.6)	1.4	2.1	2.6	2.9	0.7	2.0	3.2
3	TS$_I$**LF**-*Si*	2.8 (2.6)	0.9	1.5	6.6	1.9	3.7	2.4	1.7
4	TS$_I$**LB**-*Si*	2.9	0.7	2.4	1.5	2.9	0.7	2.5	1.5
5	TS$_I$**RF**-Re	2.3 (2.2)	2.1	1.7	4.9	2.4	1.7	2.9	0.7
6	TS$_I$**RB**-Re	5.1	<0.1	4.3	0.1	4.0	0.1	3.1	0.5
7	TS$_I$**LF**-Re	6.2	<0.1	5.2	<0.1	4.5	<0.1	3.4	0.3
8	TS$_I$**LB**-Re	4.8	<0.1	4.5	<0.1	4.2	0.1	3.0	0.6
9	ee (%)^g		**95.8 (R)**^{g}		**89.9 (R)**^{g}		**96.1 (R)**^{g}		**95.8 (R)**^{g}

^{a} Energies in kcal/mol computed at B3LYP/D95V level. ^{b} Single-point activation energy ($\Delta\Delta E^{\ddagger}$) at B3LYP/6-311++G**//B3LYP/D95V. ^{c} Single-point activation energy at B3LYP/6-311++G** level with the SCRF method based on PCM solvation model (toluene $\epsilon = 2.379$). ^{d} Energies in kcal/mol as the relative difference ($\Delta\Delta E^{\ddagger}$ or $\Delta\Delta G^{\ddagger}$) to the lowest one in each column (TS$_I$**RF**-*Si*). ^{e} In parenthesis, relative energies of the structures optimized at B3LYP/6-31G*. ^{f} Percentage of contribution of each transition state in the reaction according to the Eyring equation and Boltzmann distribution equation. Each column adds up to 100%. ^{g} Enantiomeric excess computed as Σentries(1−4) − Σentries(5−8) in each column.

arose, depending on the back (**B**) or front (**F**) orientation of the quinoline ring and the left (**L**) or right (**R**) orientation of the benzyl group (Figure 7). Additional variation arises from considering either of the two oxygen atoms of the nitro group and a *Si* or Re approach of the imine component, which led to a total of 16 transition state geometries of the **TS$_I$** type that were computed. For the remaining **TS$_{II}$** and **TS$_{III}$** type geometries, two additional sets of 8 structures each were considered in this study. The large number of atoms implied (98) in each transition state make the extensive conformational search employing triple-ζ basis set prohibitive in terms of computational cost. The preliminary search was thus conducted with the shorter D95V basis set, and the most relevant structures were further optimized at the 6-31G* level.

Among the transition structures of the **TS$_I$**-type, TS$_I$**RF**-*Si* (entry 1, Table 6) is the lowest-lying in energy at both D95V and 6-31G* computational levels and is taken as reference (0) for the energies of the rest of structures in Table 6. Thus, the **RF** arrangement of substitutents in the catalyst (benzyl group to the right and methoxy-quinoline group to the front) is preferred over the other orientations by at least 1.5 kcal/mol. According to the Eyring equation and the Boltzmann distribution equation, TS$_I$**RF**-*Si* accounts for 85−95% of the reactivity of the reaction depending on the computational variable considered ($\Delta\Delta E^{\ddagger}$ or $\Delta\Delta G^{\ddagger}$) or the introduction of larger basis sets and solvent effects (Table 6). The preferred *Si*-face attack is in accordance with the experimentally encountered formation of the R-configured product, and the comparison of the relative energies of all **TS$_I$**-type structures predicts an enantiomeric excess of 90−96% (entry 9, Table 6), which is in good agreement with the experiments. Noteworthy, reoptimization of the most favored structures at B3LYP/6-31G* level of theory did not alter significantly their geometries and relative energies (Table 6, entries 1−3, 5, data in parentheses).

Table 7. Transition State Energies and Relative Contribution Percentages for the Aza-Henry Reaction through Binding Types **II** and **III**, Computed at the B3LYP/D95V Level

entry	transition state	**TS$_{II}$** (OH···N = C)		**TS$_{III}$** (OH···O=C)	
1	TS**RF**-*Si*	0.1^a	43.1%^{b}	1.7^a	4.8%^{b}
2	TS**RB**-*Si*	2.7	0.6	2.3	1.8
3	TS**LF**-*Si*	3.4	0.2	3.2	0.3
4	TS**LB**-*Si*	3.4	0.2	4.6	<0.1
5	TS**RF**-Re	0	55.3	0	82.0
6	TS**RB**-Re	3.3	0.2	1.3	9.2
7	TS**LF**-Re	2.9	0.4	2.2	1.8
8	TS**LB**-Re	4.2	<0.1	4.2	0.1
9	ee (%)^c	**12.0 (S)**^{c}		**86.1 (S)**^{c}	

^{a} Energies in kcal/mol as the relative difference ($\Delta\Delta E^{\ddagger}$) to the lowest one in each column. ^{b} Percentage of participation of each transition state in the reaction according to the Boltzmann equation. Each column adds up to 100%. ^{c} Enantiomeric excess computed as Σentries(1−4) − Σentries(5−8) in each column.

Meanwhile, a similar analysis of the transition structures wherein the catalyst-OH is H-bonded to the imine (**TS$_{II}$** and **TS$_{III}$**, Table 7) leads to completely different results. In both cases, the TS**RF**-Re structure, which yields the wrong *S* enantiomer, is the lowest in energy and is taken as 0. When the OH group is H-bonded to the nitrogen atom (**TS$_{II}$**), the energy

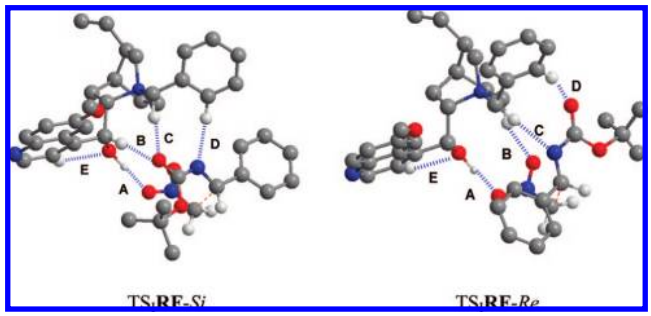

Figure 8. Structures of the two transition states lowest in energy for the aza-Henry reaction through pathway **I** calculated at the B3LYP/6-31G* level of theory.

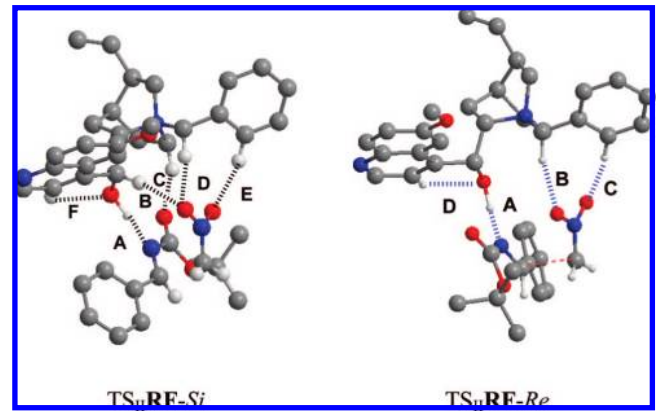

Figure 9. Structures of the two transition states lowest in energy for the aza-Henry reaction through pathway **II** calculated at the B3LYP/D95V level of theory

difference between TS$_{II}$**RF**-Re (entry 5) and TS$_{II}$**RF**-*Si*(entry 1) is minimal, and a quasi-racemic product is predicted (*S* enantiomer, 12%ee), whereas the computed ee in favor of the nonexperimental *S* enantiomer increases to 86% when the H−B is formed between the OH group and the oxygen atom of the imine. Thus, only binding mode **I** can explain the experimental enantioselectivity, which can be taken as a further proof of the OH···O$_2$N bonding during transition state.

The origin of the enantioselectivity might result from the balance of two opposite factors: on the one hand the positive interaction due to the H−B network between the different basic sites in the reactants with the OH and N$^+$−CH groups of the catalyst,[44] and on the other hand, the negative effect of the steric repulsion that arises in such bulky systems (i.e., the *t*-butyl group in the carbamate and the catalyst′s bicyclic skeleton). The lowest-lying transition state (TS$_I$**RF**-*Si*, Figure 8) presents five relatively strong H−B interactions, considering only those whose bonding distances are shorter than 2.5 Å. The shortest interaction (**A**) appears between the OH and one of the oxygens of the nitro group (1.6 Å). Another three important interactions appear between the imine-carbamate and diverse CH groups of the catalyst: **B** (2.2 Å), **C** (2.0 Å), and **D** (2.3 Å). Besides, there is an intramolecular H−B in the catalyst between the oxygen and a C−H of the pyridine ring (**E**, 2.3 Å). The fact that tight H−B interactions may be formed between the three reacting components without compromising the steric congestion seems to be the reason for the preference of that TS. As shown in TS$_I$**RF**-*Si* (Figure 8), when the imine approaches the nitronate offering the *Si* face for nucleophilic attack, the tert-butyl group points away from the catalyst′s bicycle (toward the front of our view in Figure 8), thus avoiding contact with the catalyst's methylenes.

On the other hand, the preferred transition state forming the S enantiomer (TS$_I$**RF**-Re) presents a higher energy barrier ($\Delta\Delta G^{\ddagger} \approx 2$ kcal/mol). The number of productive H−B between the carbamate and the N$^+$CH groups is reduced to two (**C** = 2.3 Å and **D** = 2.1 Å), and both are weaker than the corresponding H–B in TS$_I$**RF**-*Si*. The steric factors also play a negative role in the Re approach, difficulting optimal H-bonding contact between carbamate and catalyst.

If we consider the other two binding types (**TS$_{II}$** and **TS$_{III}$**), and following a similar reasoning, formation of the wrong *S* enantiomer would be predicted. To get the *R* enantiomer, the imine must flip over, directing the tert-butyl group toward the most congested area (TS$_{II}$**RF**-*Si*, Figure 9), whereas in the Re face attack, tert-butyl group points to the empty front side of the model (TS$_{II}$**RF**-Re, Figure 9). This effect would lead to the wrong *S* enantiomer or to a *quasi*-racemic mixture of products (Table 7).

Conclusions

An efficient catalytic asymmetric aza-Henry reaction has been realized under phase transfer conditions. This direct aza-Henry reaction holds as interesting features the validity for both nonenolizable and enolizable aldehyde-derived azomethines and the tolerance of nitroalkanes, other than nitromethane, for the production of β-nitroamines. From a synthetic point of view, the methodology described implies a direct and efficient route for the asymmetric synthesis of precursors of differently susbstituted 1,2-diamines. More interestingly, a new asymmetric synthesis of γ-amino α,β-unsaturated esters has been realized through a catalytic, highly enantioselective formal addition of β-acryloyl anion equivalents to azomethines.

Kinetic studies reveal the present reaction to be first order with respect the *N*-acyl imine, generated *in situ* from the α-amido sulfone, and the catalyst. Computational calculations at the B3LYP/6-31G* level of theory indicate that the catalyst's OH group binds preferentially to the nitro group of the nucleophile and not the electrophilic *N*-acyl imine. This is in accordance with the larger amount of charge that the nitro group presents along the reaction as compared with the charge developed by the iminic oxygen and nitrogen atoms. Thus, an optimal TS can be depicted (TS$_I$**RF**-*Si*, Figure 8) that contains a hydrogen bond network that greatly contributes to the rigidity and stability of the complex and might be one of the reasons for the high enantioselectivity of the reaction. The computed enantiomeric excess of 90−95% favoring the *R* enantiomer is in good agreement with experimental observations.

Experimental Section

General Procedure for the Aza-Henry Reaction of Nitroalkanes with α-Amido Sulfones under PTC Conditions Employing Catalyst A. To a suspension of the corresponding α-amido sulfone **1** (0.5 mmol, 1 equiv) and *N*-benzylquininium chloride **A** (27 mg, 0.06 mmol, 0.12 equiv) in dry toluene (1.5 mL) at −50 °C under a nitrogen atmosphere were successively added the corresponding nitroalkane (2.5 mmol, 5 equiv) and CsOH·H$_2$O (109 mg, 0.65 mmol, 1.3 equiv). The mixture was stirred at the same temperature for 44−54 h, then quenched with HCl (2 mL, 0.1 N), and extracted with CH_2Cl_2 (3 × 3 mL). The organic layer was washed with HCl (1 × 2 mL), dried over $MgSO_4$,

and concentrated under reduced pressure to give the crude product that was purified by flash column chromatography using mixtures of ethyl acetate/hexane as the eluent.

Acknowledgment. This work was financially supported by the University of the Basque Country (UPV/EHU) and Ministerio de Educación y Ciencia (MEC). Thanks are due to SGI/IZO-SGIker (UPV/EHU) for the generous allocation of computational resources. I.M.-M. thanks Gobierno Vasco for a predoctoral grant.

Supporting Information Available: Experimental details, analytical data and stereochemical proofs for all new compounds, kinetic experiments, Cartesian coordinates of all computed stationary points, relative and absolute activation energies for all reactions, and complete ref 35. This material is available free of charge via the Internet at http://pubs.acs.org.

JA800253Z

(44) For X-Ray evidence of a H-bond network in a tetrabutyl ammonium cation, see: Reetz, M. T.; Hüette, S.; Goddard, R. *J. Am. Chem. Soc.* **1993**, *115*, 9339–9340.